

# Petrography and geochemical framework of guébaké dolerites dyke swarms (north Cameroon, central Africa)

Abondou Togo <sup>1\*</sup>, Nkouandou Oumarou Faarouk <sup>2</sup>, Zangmo Tefogoum.Ghislain <sup>1</sup>, Fagny Mefire Aminatou <sup>1</sup>, Daouda Dawai <sup>1</sup>, Dinamou Appoliaire <sup>2</sup>, Guihdama Dagwai Justin <sup>1</sup>, Adama Haman <sup>2</sup>

<sup>1</sup> Department of Earth Sciences, Faculty of Sciences, University of Maroua, P.O. Box 46 Maroua, Cameroon

<sup>2</sup> Department of Earth Sciences, Faculty of Science, University of Ngaoundéré, P.O. Box 454 Ngaoundéré Cameroon

\*Corresponding author E-mail: [togo.abondou@yahoo.fr](mailto:togo.abondou@yahoo.fr)

## Abstract

Dolerites dykes of 4.5 to 25 m wide extend from 200m to 1km, crosscut the Guébaké granitoids basement in northern Cameroon along EW to N100E directions. Petrographic studies reveal the microlitic porphyritic texture to classical doleritic texture of ophitic to sub-ophitic types. Guébaké dolerites are mainly composed in various proportions of skeletal plagioclase and feldspar, clinopyroxene, amphibole and oxides crystals. ICP-MS and ICP-AES geochemical analyses have distinguished a lava series composed of trachybasalts, basaltic trachyandesites, trachyandesites, trachytes and rhyolites of continentale tholeiites affinity. Lavas have been differentiated through fractional crystallization process coupled with crustal contamination and metasomatism. Guébaké dolerites are products of relatively high partial melting rate of E-MORB mantle component. They stand as fingerprints of the post pan African crustal consolidation and precursor of the development of central African rift system at Cretaceous times.

**Keywords:** Dolerites; Petrology; Continental Tholeiite; Post Pan African; Benue Valley; Cameroon.

## 1. Introduction

Geodynamical evolution of Pan African mobile belt is very complex due to multiple conjugaison and superimposition of tectonic events which occurred through geological times with a strong imprint of the Neoproterozoic events (Toteu et al., 2004). In Central Africa, especially in Cameroon territory, the Central Pan African Belt (CPAB) according to Toteu et al. (2004) has benefited from the many geological and geochronological studies (Toteu, 1990 ; Toteu et al., 1994, 2004, 2006 a and b ; Ngako et al., 2008 ; Ganwa et al., Tchakounté et al., 2017) which have led to several geodynamical models involving or not the main African cartons (Ngako et al., 2008 ; Toteu et al., 2004 ; Ngako and Njonfang, 2011 and Tchakounté et al., 2017). From those tectonic events might arise the mantle-crust disequilibrium favouring the occurrence of volcanic and subvolcanic rocks which are considered as fingerprints relative to tectonic event. In the northern domain of Pan African belt (Toteu et al., 2004), those rocks occurred as dolerite dykes cutting the Pan African basement or as alkali lava flows interbedded with sedimentary strata (Guiraud and Maurin, 1992 ; Ngounouno et al., 2001). The reconstitution of the geodynamic evolution of Pan African belt still complex and should be improved by detail studies carried out on key tectonic elements as dolerite dykes or sills (Srivastava, 2010) for the best understanding of the belt. Moreover, mafic dolerite dyke swarm provide an important means of tracking major periods of continental rifting and supercontinent fragmentation and may represent part of the magmatic plumbing system of the continental flood basalts (Ernst et al., 1995).

This work aims to provide the petrography and geochemistry framework on Guébaké dolerite dykes in view to have preliminary informations on their composition, the nature of mantle source and discuss their relevance on the tectonic reconstitution of it tectonic setting.

## 2. Geological setting

Dolerite dykes widespread in Guébaké locality in Benue valley, the northwestern branch of Yola trough (Figure 1), in Cameroon territory. Guébaké basement belongs to northern domain of Pan African chain (Toteu et al., 2004) also called West Cameroon Domain (WCD), limited to Adamawa domain by Tcholliré–Banyo shear zone (figure 1) at the south, in the center by Maroua-Poli and Godé-Gormaya shear zones closed to Nigeria-Cameroon boundaries. WCD is affected by two main deformation phases (Toteu et al., 2004). The first is marked by a flat-lying foliation associated with isoclinal folds, rotational structures of garnet and a N110°–N140° stretching lineation (Toteu et al. 2004). The second is characterized by the development of tight and upright folds with vertical axial plane foliations. Dyke unites crosscut the basement of Garoua basin consisting of recent plutonic intrusion of biotite bearing granite and migmatite (Koch, 1959). Recent studies (Toteu et al., 2004) have distinguished the Neoproterozoic medium- to high-grade schists and gneisses, pre-syn to post Pan African tectonic granitoids of 580 to 660 Ma (Toteu et al., 2001). All those formations exhibit the same characteristics feature with the schists and gneisses of northeastern Nigeria basement (Ferré et al. 2002). The basement rocks are covered by Hauterivian-early Aptian sediments of E-W Aptian-Albian half-grabens which are underlined by WNW-ESE striking faults (Guiraud and Maurin, 1991). Wilson and Guiraud (1992)



have reported the occurrence of interstratified alkali basalt flows, associated with numerous dolerite dykes and sills of N70° to E-W direction, parallel to the basin boundary faults. Dolerite dykes should have the minimum age of 80 Ma.

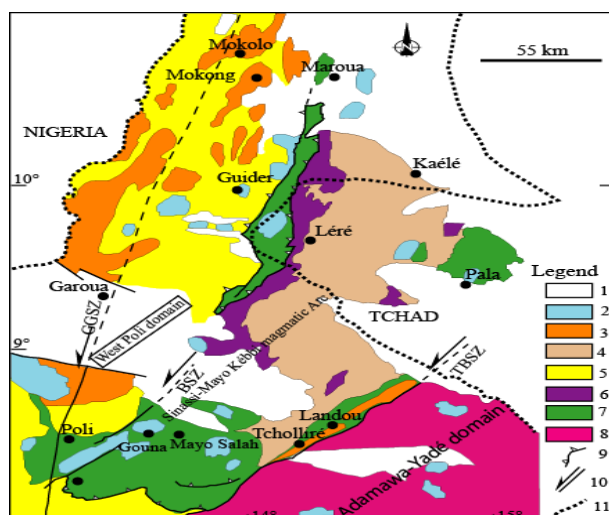


**Fig. 1:** Geological sketch map of northern Cameroon (modified from Penaye et al., 2006) : (1) post-pan African sediments ; (2) Late to post-tectonic Pan-African granitoids ; (3) syntectonic granite ; (4) Mayo-Kebbi batholith : Tonalite, trondhjemite and granodiorite ; (5) medium-to high-grade gneisses of the NW-Cameroon domain ; (6) mafic to intermediate complex of the Mayo-Kebbi domain (metadiorite and gabbro-diorite) and amphibolite ; (7) Neoproterozoic low to medium-grade volcano-sedimentary sequences of the Poli-Léré group ; (8) remobilized Palaeoproterozoic Adamawa-Yadé domain ; (9) thrust front ; (10) strike-slip fault : TBSZ=Tcholliré-Banyo Shear Zone ; GGSZ=Godé-Gormaya Shear Zone ; (11) state border.

### 3. Analytical methods

Ten thin polished sections have been made from the selected representative samples at the University of Yaoundé 1. ICP-MS and ICP-AES analytical methods have been used to determine major, trace and rare earth elements at ACMEL Analytical Laboratories, Vancouver, British Columbia, Canada. Major and trace elements were carried out from pulps. 0.2 g of rock powder was fused with 1.5 g  $\text{LiBO}_2$  and then dissolved with 4 acid digestions. Analytical precisions vary from 0.04 to 0.1 for major elements; from 0.1 to 0.5 ppm for trace elements; and from 0.01 to 0.5 ppm for rare earth elements. Loss On Ignition (LOI) has been determined by weight difference after ignition at 1000 °C.

## 4. Results

### 4.1. Fieldwork and petrography

Field studies carried out on dolerite dyke swarm of Guébaké have distinguished numerous dykes of E-W to N100E directions (Figure 2A and 2C), cutting the granitic rocks of the basement. Individual dolerite dyke varies in width from 4.5 to 25m and are extend along strike from 200 to more than 1km (Figure 2A and 2C). The majority of dolerite dykes overhang the topography up to 1.5 m (Figure 2A). Dolerite exhibit sharp contacts with the granitic basement and apophyse structures of finger-like feature propagate sometimes into the granitic at the edges (Figure 2E). Dykes are organized in angular blocks of 30 to 80cm with some dykes showing few ovoid bowls of 25 to 50 cm in diameter. Hand specimens of representative samples show dark matrix covered by thin (< 1cm) whitish patina of aphyric to porphyritic textures (Figures 2B and 2D) or mesocrate matrix of coarse grain structure (Figures 2B). Whitish feldspar of 2 to 5 mm (10 to 20 vol. %) and angular blackish minerals (5 to 10 vol. %) are distinguished in the matrices. Fragments of 3 to 8 cm of granitic composition are frequent in some outcrops.



**Fig. 1:** 4.5-7.5m Guébaké dolerite dykes trending EW (A) with coarse structure (B) and N100E (C) with plagioclase phenocrysts in blackish matrix (D). E : Doleritic apophysis of 30 cm showing sharp contact with granite of the basement.

On plate polarized light, Guébaké dolerite show two variable textures, microlitic porphyritic (Figure 3A, 3B and 3D) and classical doleritic textures of intersertal (Figure 3C) to sub-ophitic types (Figure 3D). All dolerite types are composed of phenocrysts and microliths of K-feldspar, plagioclase, clinopyroxene, amphibole and microcrysts of oxides. K-feldspar and plagioclase phenocrysts are skeletal in shape and include or contain microcrysts of oxides (Figure 3C, 3D, 3E) in borders (Figure 3F). Clinopyroxene phenocrysts are intimately linked to those of oxides and look skeletal (Figure 3C, 3D, 3E). Some clinopyroxene crystals might have destabilized into oxides phenocrysts



(Figure 3C, 3E). All those crystals present the entire or partial inclusion of oxides microcryst and minute crystals of elongated plagioclase microliths. Few percent (< 10 %) of amphibole phenocrysts are heuhedral in shape (Figure 3) and some might have been proceeded from clinopyroxene destabilization (Figure 3C). Two generation of oxides crystals are present in Guébaké dolerites: (1) Magmatic oxides with various sides and features, sometimes included in phenocrysts and (2), inherited oxides proceeded from altered clinopyroxene crystals (Figure 3E).

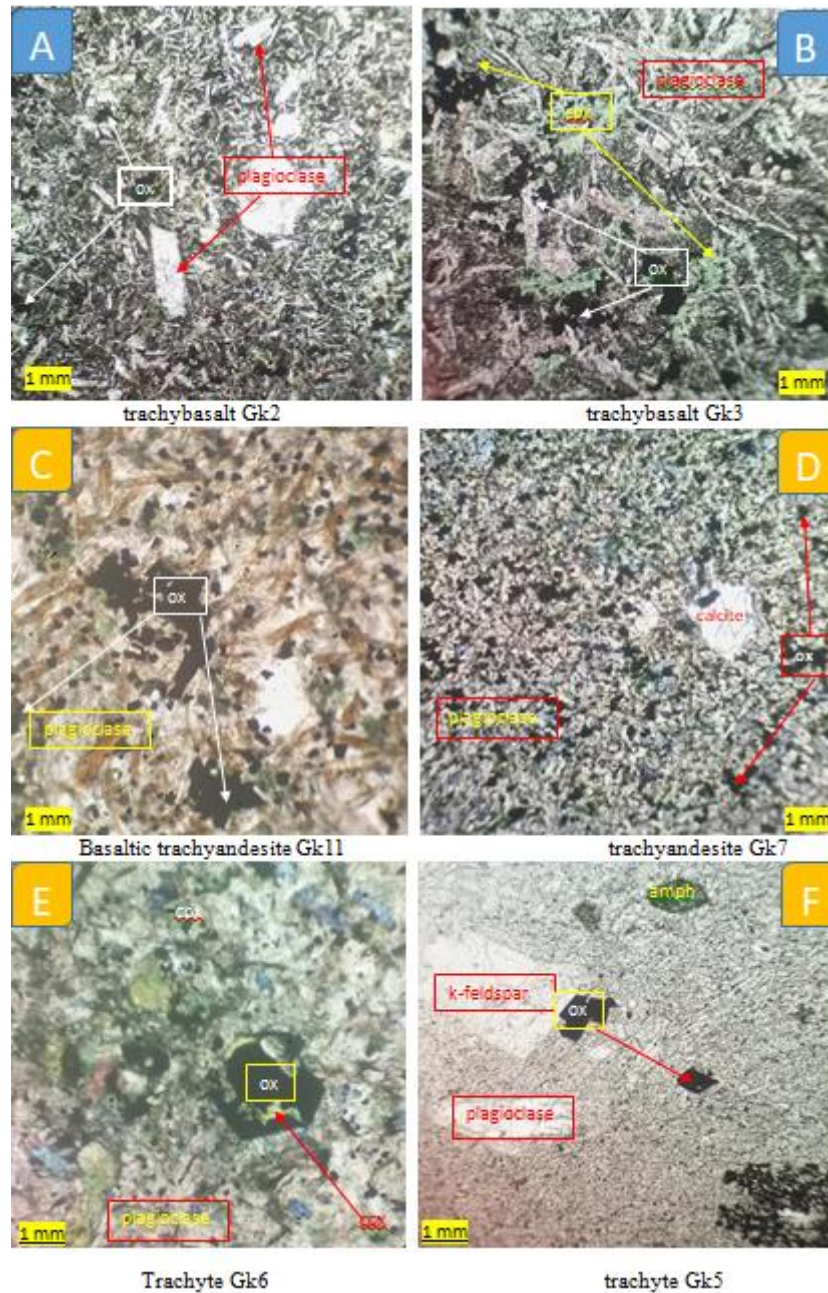


**Fig. 3:** Microlitic porphyritic (A, D, E) and classical doleritic (B, C, E) textures of Guébaké dolerites showing skeletal plagioclase and clinopyroxene crystals in ophitic textures (B, C), altered clinopyroxene in oxides crystals (C, E) and oxides-feldspar association (F) in trachyte.

#### 4.2. Geochemical characteristics

Geochemical analyses of Guebaké representative dolerites are presented in table 1. Lavas are distinguished as trachybasalts, basaltic trachyandesite, trachyandesite, trachydacite and rhyolite after the IUGS classification scheme (Figure 4, Le Maître, 2002).

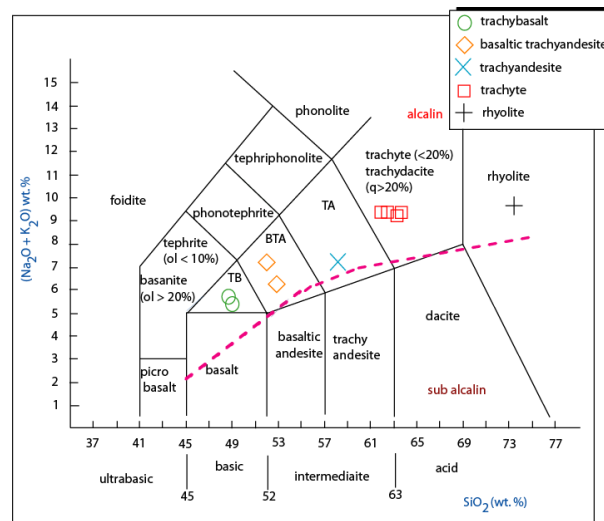


**Fig. 4:** Nomenclature of Guebaké dolerites using TAS diagram of Le Maître (2002). Pink dashed line separates alkaline and sub alkaline fields (After Miyashiro, 1978).

**Table 1;** ICP-AES and ICP-MS geochemical analyses of Guébaké dolerites. Major elements have been recalculated to 100%. TB: Trachybasalts, BTA: Basaltic Trachyandesite, TA: Trachyandesite

sample	TB	TB	BTA	BTA	TA	trachyte	trachyte	trachyte	trachyte	rhyolite
SiO <sub>2</sub>	48.75	49.04	52.03	52.88	58.19	61.94	62.51	63.39	63.73	73.44
TiO <sub>2</sub>	3.24	3.22	2.07	2.72	1.94	0.96	0.93	0.90	0.90	0.15
Al <sub>2</sub> O <sub>3</sub>	15.33	15.29	16.64	16.10	15.90	16.67	16.64	16.77	16.57	13.17
Fe <sub>2</sub> O <sub>3</sub>	14.28	14.05	10.35	11.66	9.00	6.30	6.03	5.01	5.01	2.93
MnO	0.18	0.19	0.15	0.15	0.11	0.11	0.10	0.09	0.09	0.09
MgO	4.57	4.61	3.97	3.47	2.13	1.27	1.16	1.26	1.23	0.06
CaO	6.88	7.20	6.95	6.24	4.79	2.98	2.88	3.04	2.78	0.43
Na <sub>2</sub> O	3.48	3.58	3.35	3.69	3.56	4.54	4.43	4.56	4.92	5.06
K <sub>2</sub> O	2.23	1.78	3.85	2.56	3.70	4.84	4.94	4.66	4.45	4.62
P <sub>2</sub> O <sub>5</sub>	1.07	1.05	0.67	0.53	0.67	0.38	0.37	0.31	0.31	0.03
sum	100.00	100.00	100.00	100.00	100.00	100.00	100.00	100.00	100.00	100.00
Quartz	0.00	0.79	0.00	3.73	10.40	8.40	9.54	10.57	10.26	0.00
Plagioclase	49.54	51.19	47.66	51.44	46.86	49.44	48.62	50.23	51.80	42.12
Orthoclase	13.30	10.64	22.87	15.25	22.04	28.72	29.31	27.66	26.42	27.36
Diopside	6.14	6.94	9.06	6.34	2.44	1.25	0.79	1.32	1.50	1.71
Hypersthene	15.26	15.03	6.77	11.19	8.67	6.44	6.19	5.39	5.18	1.81
Olivine	0.16	0.00	3.15	0.00	0.00	0.00	0.00	0.00	0.00	0.00
Acmite	0.00	0.00	0.00	0.00	0.00	0.00	0.00	0.00	0.00	0.69
Ilmenite	6.21	6.17	3.95	5.20	3.70	1.84	1.77	1.71	1.73	0.28
Magnetite	6.90	6.79	4.99	5.63	4.34	3.03	2.90	2.41	2.41	1.06
Apatite	2.50	2.46	1.55	1.23	1.55	0.88	0.86	0.72	0.72	0.07
Mg	32.45	32.89	35.83	31.12	26.99	24.35	23.50	28.13	27.66	3.50
Be (ppm)	3	6	7	1	2	2	2	3	3	5
Ba	1031	862	1001	844	1285	1611	1686	1472	1426	15
Ni	38	34	<20	23	<20	<20	<20	<20	<20	<20
Sc	25	24	23	17	12	9	8	8	8	2
Co	41.5	40.0	28.4	35.2	22.5	5.8	5.9	5.9	4.9	1.0
Cs	2.2	1.5	1.2	2.0	1.7	1.6	1.4	2.2	1.0	2.2
Ga	20.6	20.5	19.1	22.5	21.4	23.3	23.6	21.9	22.7	31.2
Zr	378.9	368.8	277.8	307.9	383.0	462.4	477.2	389.6	399.5	717.0
Hf	8.8	8.6	7.1	8.0	9.5	11.8	12.2	9.7	10.0	23.8
Ta	1.2	1.2	0.7	1.3	1.5	1.7	1.8	1.2	1.2	5.1
Nb	21.6	20.8	11.9	21.4	23.4	28.5	30.1	18.9	19.6	85.0
Rb	66.5	52.4	130.7	75.7	109.6	129.4	135.1	145.9	117.8	279.0
Sn	2	2	3	2	3	3	2	2	3	7
Sr	578.8	543.0	632.9	656.9	682.7	535.5	533.2	587.3	561.0	8.9
Ta	1.2	1.2	0.7	1.3	1.5	1.7	1.8	1.2	1.2	5.1
Th	2.4	2.2	10.4	6.1	14.9	19.2	19.8	29.4	30.2	42.3
U	0.6	0.5	2.1	1.0	1.8	2.3	2.3	2.6	2.8	6.5
V	249	246	265	176	120	20	17	32	29	<8
W	0.7	<0.5	0.8	0.5	0.7	0.8	0.8	1.1	6.0	<0.5
Zr	378.9	368.8	277.8	307.9	383.0	462.4	477.2	389.6	399.5	717.0
Y	44.8	42.8	24.5	27.7	30.2	31.8	32.1	25.0	25.6	67.4
La	46.9	46.5	35.3	43.7	67.6	74.1	74.7	78.2	79.7	91.1
Ce	105.2	104.1	75.0	91.0	133.3	143.4	144.6	147.6	151.7	189.6
Pr	13.8	13.4	9.6	11.2	15.4	16.5	16.5	15.8	16.4	21.5
Nd	59.7	57.6	40.2	44.5	59.1	60.9	60.8	56.1	59.2	75.3
Sm	11.7	11.6	7.6	8.7	10.3	10.7	10.8	9.3	9.7	15.6
Eu	3.2	3.2	2.2	2.6	2.7	2.8	2.8	2.4	2.4	0.2
Gd	11.3	10.9	6.4	7.8	8.7	8.4	8.7	7.2	7.5	13.5
Tb	1.6	1.5	0.9	1.1	1.1	1.2	1.2	1.0	1.0	2.2

Dy	8.7	8.4	4.8	5.9	5.8	6.2	6.3	5.1	5.2	12.3
Ho	1.7	1.6	0.9	1.0	1.1	1.2	1.2	0.9	0.9	2.5
Er	4.7	4.4	2.5	2.8	3.0	3.1	3.3	2.5	2.5	6.8
Tm	0.6	0.6	0.4	0.4	0.4	0.5	0.5	0.3	0.4	1.0
Yb	4.0	3.8	2.2	2.3	2.6	2.8	2.9	2.0	2.2	6.5
Lu	0.6	0.5	0.3	0.3	0.4	0.4	0.4	0.3	0.3	0.9
Zr/Hf	43.1	42.9	39.1	38.5	40.3	39.2	39.1	40.2	40.0	30.1
Nb/Ta	18.0	17.3	17.0	16.5	15.6	16.8	16.7	15.8	16.3	16.7
Y/Nb	2.1	2.1	2.1	1.3	1.3	1.1	1.1	1.3	1.3	0.8
TbN/YbN	1.7	1.7	1.8	2.1	2.0	1.9	1.8	2.1	2.0	1.5
CeN/YbN	6.8	7.0	9.0	10.4	13.4	13.4	12.9	18.7	17.9	7.5

Major elements distribution (Figure 5) using SiO<sub>2</sub> as differentiation index shows the decrease variations of TiO<sub>2</sub>, MgO, CaO and P<sub>2</sub>O<sub>5</sub> contents while Na<sub>2</sub>O and K<sub>2</sub>O contents exhibit the increase variations. Al<sub>2</sub>O<sub>3</sub> oxide shows a contrast variation. CaO/Al<sub>2</sub>O<sub>3</sub> ratios are low and vary between 0.2 and 0.5 with rhyolite lava having the lowest value (0.03). Mg# (=100\*(MgO/40.32)/(MgO/40.32+FeOt/71.87)) decrease from trachybasalt to rhyolite (32.5 to 3.5).

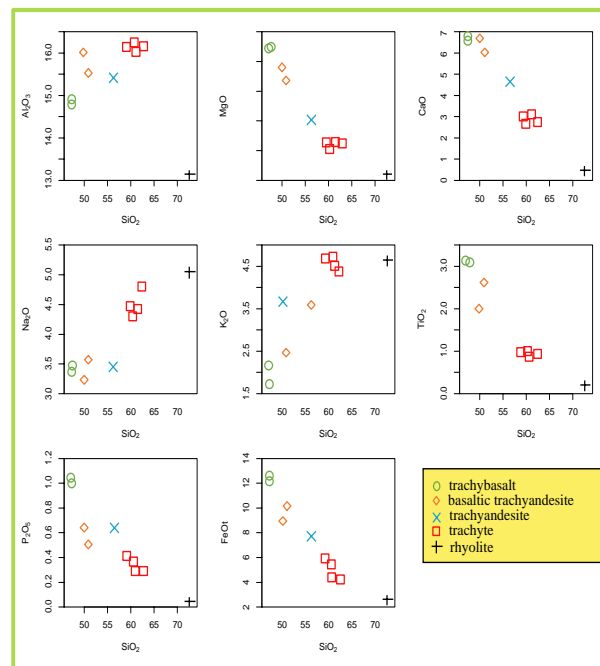


**Fig. 5:** Harker diagrams showing compositional variations of Guébaké dolerites using major oxides contents.

Norm calculations show that Guébaké dolerites are saturated to oversaturated lavas with 0 to 10.5 % of quartz contents (Table 1). Basaltic lavas (trachybasalts and basaltic trachyandesites) are saturated to relatively oversaturated (0 to 3.373 normative quartz %). Transitional elements Ni, Co, Cr and V contents are low and decrease from trachybasalt to rhyolite. Alkali element Rb contents increase from trachybasalts (52.4-130. Ppm) and basaltic trachyandesite to rhyolite (29.0 ppm) while alkali earth elements contents Sr decrease (563.0-682.7 ppm to 8.9 ppm) and Ba (862-1031 ppm to 15 ppm). Zr (277.8 to 717 ppm) and Hf (7.1 to 23.8 ppm) contents relatively increase from basaltic to differentiated lavas, leading to relatively constant ratios (38.5-43.1) of Zr/Hf. Low Zr/Hf ratios are found in rhyolite (30.1). Nb contents (20.8-21.4 ppm) are constant in basaltic lavas (trachybasalts and basaltic trachyandesite) excepted BTA GK11 (11.9 ppm). Nb contents (23.4 ppm) are relatively high in trachyandesite. Trachyte show contrast variations: Nb contents (28.5-30.1 ppm) are high in trachyte GK9 and GK8 respectively compared to trachyte GK6 and GK5 with are characterized by low and constant values (18.9-19.6 ppm) of this element. Very high Nb contents are found rhyolite (85.0 ppm). Ta contents show similar variation (Table 1). Nb/Ta ratios are relatively constants in all lavas (15-18). Th contents are low in trachybasalts (2.2-2.4 ppm) and increase from BTA (6.1 ppm) to rhyolite (42.3 ppm). Values of Th/Yb (0.6) and Ta/Yb (0.3) ratios are low in trachybasalt and basaltic trachyandesite GK11, and vary between 2.7 and 6.9 in others lavas. High values of Th/Yb (13.8-14.4) are found in trachyte GK5 and GK6. Ta/Yb (0.5-0.8) ratios are low and relatively constant in all lavas. Y contents are high in TB (42.8-44.8 ppm) and rhyolite (67.4 ppm). Y contents are less than 30.0 ppm in the rest of lavas. Y/Nb ratios are high in basalts (2.0). Y/Nb values are low (1.1 to 1.3) in others lavas and very low value is found in rhyolite (0.8). Spider diagram (Figure 6a) shows general decreasing patterns from incompatible to compatible elements. Negative are noticed in Nb, Ta, P and Ti. TB are characterized by negative anomalies in Th and U. Normalized rare earth elements (Figure 6b) are more than 50 times the mantle values for La. More than 100 times as great as that of the mantle values in these elements characterize trachyte and rhyolite lavas. CeN/YbN ratios are slightly low (4-9) but high in rhyolite (14). Normalized TbN/YbN ratios are low (1.7-2.1) and relatively constants in all lavas while low value of these ratio (1.5) are found in rhyolite.

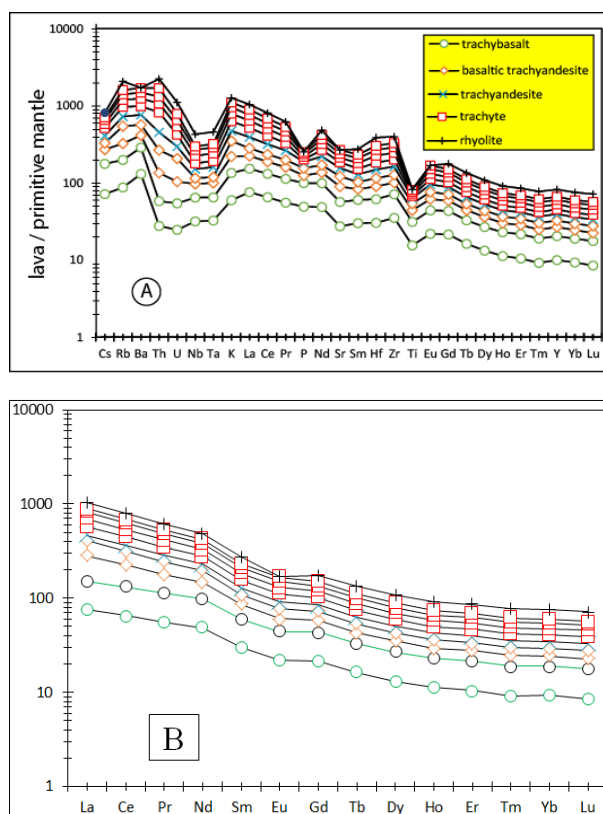


Fig. 6: Normalized multielements diagram (A) and REE (B) of Guébaké dolerites (After McDonough and Sun, 1995).

## 5. Discussions

Guébaké dolerite dyke swarm crosscut the pan African granitic basement of Benue valley of northern Cameroon thus belong to the post pan African formations. The occurrence of Guébaké dyke swarm should be linked to the late pan African crustal consolidation which have produced major basement lineaments and faults during extensional tectonic even which have favoured the opening of the West and Central Africa Rift System (WCARS) where rifted basins evolved in five major tectonic phases (Genik, 1972; Guiraud and Maurin, 1992). Reminding that dyke orientations are EW or N100E, which are the main major directions of small basins located in central and northern Cameroon (Guiraud and Bosworth, 1997), opened in response to a sub meridian extensional regime, from Neocomian to Early Aptian period (Guiraud and Maurin, 1992). These ideas suggest that doleritic magma have filled the pan African cracks as attested the sharp contacts between doleritic magma and granitic of the basement (Figure 2E) so as the occurrence of the apophyse structures propagating into the granitic (Campbell, 1985). Magma flow should be turbulent and dolerite may have undergone the crustal contamination process as the flowing magma might have eroded the walls of the basement and the magma become contaminated with crustal material (Campbell, 1985). The occurrence of granitic fragments of centimeters side and the width of individual dyke of more than 3 m (up to 25 m) are strong arguments in favour of magma contamination through turbulent flow (Campbell, 1985). It has been suggested that dyke swarms associated with plumes tend to be thicker, averaging 20 to 40 m (Ernst et al., 1995). Guébaké dykes with widths of 4 to 30 m are thus supposed to be related to mantle plume occurrence under the studied area. This suggestion is enhanced by the uplift feature of the Benue valley of northern Cameroon as supported by gravity and seismic studies (Fairhead and Okereke, 1988; Poudjom Djomani et al., 1997). Petrography studies carried out on Guébaké dolerites exhibit scrawny minerals attesting of fluids perturbation so as the occurrence of hydrous minerals (calcite and amphibole). Geochemical analyses distinguish the series of lavas probably differentiated through fractional crystallization process as attested the continuous variation of oxides contents (Figure 5) coupled with the decreasing values of Mg#. Contribution of feldspar and apatite are noticed if one considers the weak P, Sr and Eu negative anomalies respectively on Figure 6A and 6B. Guébaké dolerites should be within plate lavas (Figure 7) of continental tholeiites composition (Figure 8).

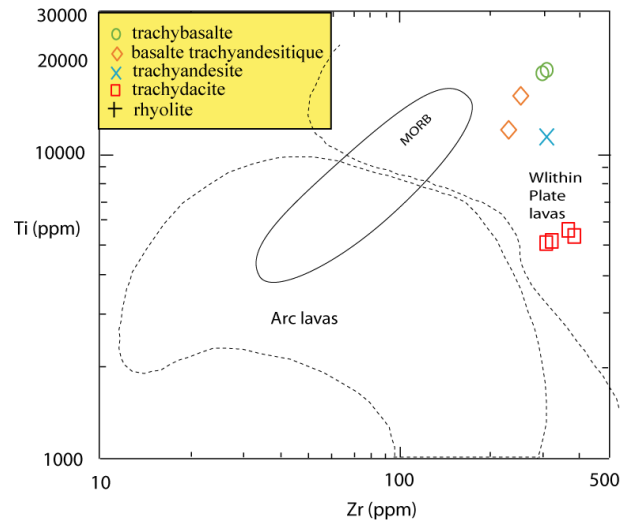


Fig. 7: Ti Vs Zr (in ppm) after Pearce (1982) of Guébaké dolerites in the field of within plate lavas. Same symbole as in Figure 4.

This suggestion is ascertained by Nb, Ta and Ti anomalies (Dupui and Dostal, 1988) shown by spider diagram (Figure 6A) and high Y/Nb ratios of basaltic lavas. Low CeN/YbN of basaltic lavas suggest the high partial melting rate of the mantle source. Relatively constants ratios of Zr/Nb and Nb/Ta attest that all lavas belong to the same lava series.

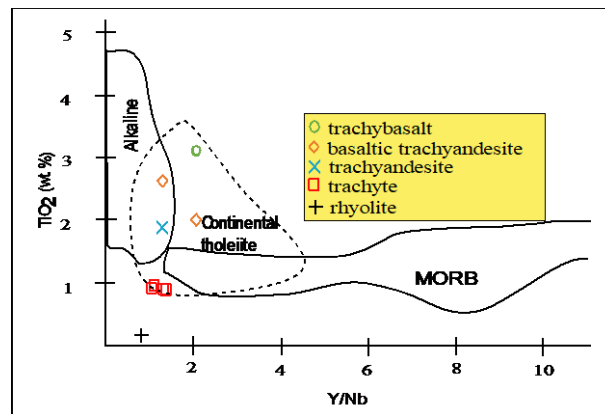


Fig. 8: Composition of dolerites Guébaké Plotted in TiO<sub>2</sub> Vs Y/Nb diagram discrimination after Floyd and Winchester (1975).

The relatively high ratios of Zr/Nb of basaltic trachyandesite (GbK11), trachyte GK5 and GK6 suggest that those lavas have been more contaminated by crustal materials. Guébaké dolerites mantle source should be E-MORB mantle component (Figure 9) of spinel-bearing composition as deduced from Figure 10 and lavas should have experienced the deep crustal recycling (Figure 9).

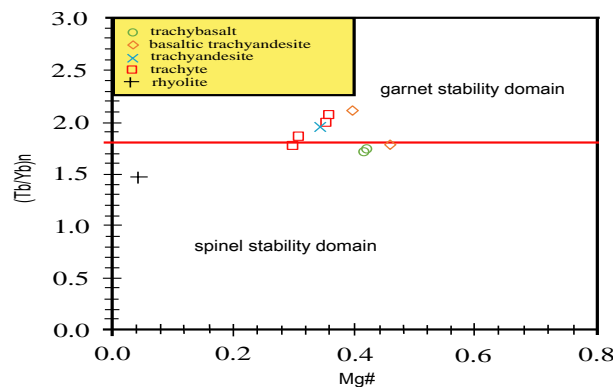
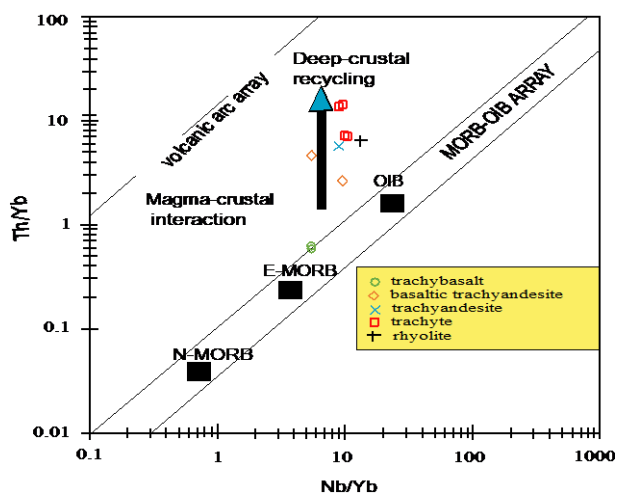


Fig. 9: (Tb N/Yb N) vs. Mg# diagram of Guébaké dolerites after Wang et al. (2002). Tb and Yb are normalized according to McDonough and Sun (1995).





**Fig. 10:** Th/Yb Vs Nb/Yb diagram after Pearce (2008). Guebaké dolerites are plotted close to the E-MORB mantle source and evolve toward the deep-crustal recycling field.

Geodynamic setting of Guébaké dolerites is given by ternary diagrams where basaltic lavas are plotting closed to the field of E-MORB (Figure 11A) and within the continental tholeiite domain (Figure 11B). The rest of the lavas are plotted in the field of volcanic arc basalts (Figure 11A) and orogenic basalts (Figure 11B). This suggestion is likely if one considers that Guébaké dolerites belong to Yola branch of Benue trough (Figure 1), part of Central Africa Rift System (CARS, Genik, 1992). Therefore, the location of the majority of Guébaké dolerites in the field of volcanic arc and orogenic basalts is due to crust-magma interaction. Guébaké dolerites are thus considered as times markers of post pan African crustal consolidation, whose faults formed precursor of Central African rift system at Cretaceous times.

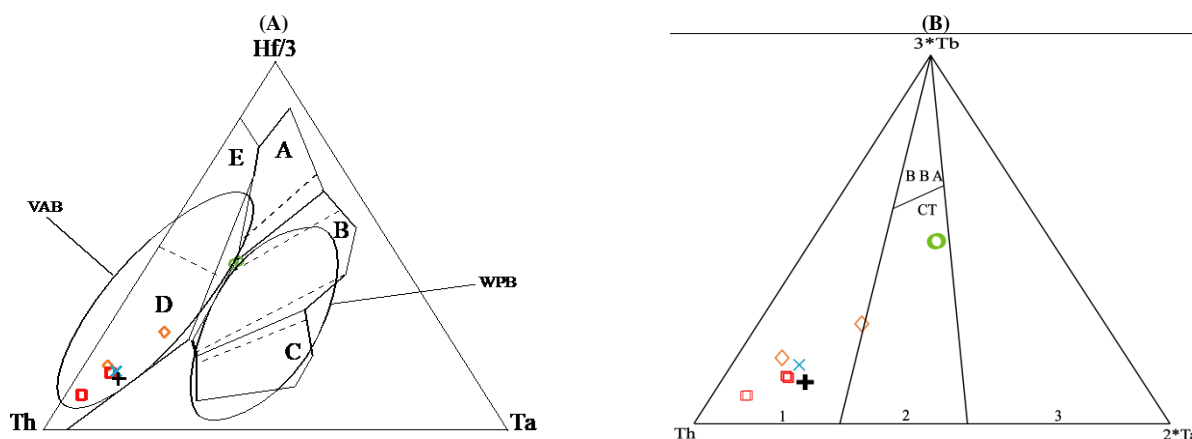


**Fig. 11:** Guebaké dolerites in geodynamic diagrams A: Hf/3-Th-Ta diagram after Wood (1980). A: N-MORB; B: E-MORB; C: Alkali domain; D: Volcanic Arcs Basalts of Hf/Th>3.0 and E: Calco-Alkali basalts domain with Hf/Th <3.0 and (B). Composition of studied dolerites plotted in (Th-3Tb-2Ta) after Cabanis and Thieblemont (1988), BAB: Back Arc Basin Basalts, CT: Continental Tholeiites; 1. Orogenic Basalts, 2. Continental Tholeiites and Arc Basin Basalts and 3. Nonorogenic Basalts.

## 6. Conclusion

Dolerite lavas occur at Guébaké locality in Benue basin of north Cameroon as 4.5 to 25m dykes, crosscutting the granitoides of the basement along EW to N100E directions. Individual dyke is organized in blocs of 25 to 80cm and composed of feldspar, plagioclase, clinopyroxene and oxides. Guébaké dolerites are microlitic porphyritic and classical doleritic textures of intersertal to sub-ophitic types. Geochemical analyses distinguish the lava series composed of trachybasalts, basaltic trachyandesites, trachyandesites, trachytes and rhyolites of continental tholeiite affinity. Doleritic magmas are the result of relatively high partial melting rate of E-MORB mantle source and resulted magmas have undergone the deep crust-magma interaction. Guébaké dolerites stand as fingerprints of the post pan African crustal consolidation whose faults formed precursor of central African rift system at Cretaceous times.

## Acknowledgments

Authors greatly thank the “AcmeLab” for geochemical analyses. This paper is part of Abondou Togo thesis. Blind reviewers are thanked for the strong improvement of this paper.

## References

- [1] Bryan SE & Ernst RE (2008) Revised definition of Large Igneous Provinces (LIPs). *Earth Science Reviews* 86 (1-4), 175-202. <https://doi.org/10.1016/j.earscirev.2007.08.008>.
- [2] Cabanis B & Thieblemont D (1988) La discrimination des tholéiites continentales et des basaltes arrière-arc. Proposition d'un nouveau diagramme Th-Tbx3-Tax2. *Bulletin de la Société Géologique de France* 8 (IV, 6), 927-935. <https://doi.org/10.2113/gssgfbull.IV.6.927>.



- [3] Campbell IH (1985) the difference between oceanic and continental tholeiites: A fluid dynamic explanation. *Contribution to Mineralogy and Petrology* 91, 37-43. <https://doi.org/10.1007/BF00429425>.
- [4] Dupuy C & Dostal J (1984) Trace element geochemistry of some continental tholeiites. *Earth and Planetary Science Letters* 67, 61-69. [https://doi.org/10.1016/0012-821X\(84\)90038-4](https://doi.org/10.1016/0012-821X(84)90038-4).
- [5] Ernst RE, Head JW, Parfitt E, Grosfils E & Wilson L (1995) Giant radiating dyke swarms on Earth and Venus. *Earth-Science Reviews* 39, 1-58. [https://doi.org/10.1016/0012-8252\(95\)00017-5](https://doi.org/10.1016/0012-8252(95)00017-5).
- [6] Fairhead D & Okereke CS (1988) Depths to major density contrast beneath the West-African rift system in Nigeria and Cameroon based on the spectral analysis of gravity data. *Journal of African Earth Sciences* 7 (5/6), 769-777. [https://doi.org/10.1016/S0899-5362\(00\)00058-0](https://doi.org/10.1016/S0899-5362(00)00058-0).
- [7] Fairhead JD (1988) Mesozoic plate tectonic reconstructions of the central South Atlantic Ocean – The role of the West and Central African Rift system in Nigeria and Cameroon and its tectonic interpretation. *Tectonophysics* 143, 141-159. [https://doi.org/10.1016/0040-1951\(92\)90255-5](https://doi.org/10.1016/0040-1951(92)90255-5).
- [8] Ferré EC, Gleizes G & Caby R (2002) Tectonic and post-collisional granite emplacement in a obliquely convergent orogen: the trans-Saharan belt, Ester Nigeria. *Precambrian Research* 114, 199-219. <https://doi.org/10.1144/gsjgs.153.5.0719>.
- [9] Ganwa AA, Frisch W, Siebel W, Shang KC, Mvondo Ondo J, Satir M & Tchakounté NJ (2008b) Zircon 207Pb/206Pb evaporation ages of Panafrican metasedimentary rocks in the Kombé-II area (Bafia Group, Cameroon): Constraints on protolith age and provenance. *Journal African Earth Sciences* 51, 77-88. <https://doi.org/10.1016/j.jafrearsci.2007.12.003>.
- [10] Genik GJ (1992) Regional framework, structural and petroleum aspects of rift basins in Niger, Chad and the Central African Republic (C.A.R.). *Tectonophysics* 213, 169-185. [https://doi.org/10.1016/0040-1951\(92\)90257-7](https://doi.org/10.1016/0040-1951(92)90257-7).
- [11] Guiraud R & Bosworth W (1997) Senonian basin inversion and rejuvenation of rifting in Africa and Arabia: synthesis and implications to plate-scale tectonics. *Tectonophysics* 282 39-82. [https://doi.org/10.1016/S0040-1951\(97\)00212-6](https://doi.org/10.1016/S0040-1951(97)00212-6).
- [12] Guiraud R & Maurin JC (1991) Le rifting en Afrique au Crétacé inférieur : Synthèse structurale, mise en évidence de deux étapes dans la genèse des bassins, relation avec les ouvertures océaniques panafricaines. *Bulletin de la Société Géologique de France* 1962, 811-823. <https://doi.org/10.2113/gssgfbull.162.5.811>.
- [13] Guiraud R & Maurin JC (1992) Early Cretaceous Rifts of Western and Central Africa: an overview, In: P.A. Ziegler: (Editor). *Geodynamics of Rifting, Volume II. Case I history studies on Rifts: North and South America, Africa-Arabia*. *Tectonophysics* 213, 153-368. [https://doi.org/10.1016/0040-1951\(92\)90256-6](https://doi.org/10.1016/0040-1951(92)90256-6).
- [14] Koch P. 1959. Carte géologique de reconnaissance à l'échelle du 1/500000, République du Cameroun. Garoua-Ouest, Direction des Mines et Géologie, Cameroun, Paris
- [15] Le Maitre RW (2002) *Igneous Rocks: A classification and glossary of terms. Recommendations of the IUGS Sub-Commission on the Systematics of Igneous Rocks*, 2nd edition. Cambridge University Press, Cambridge. <https://doi.org/10.1017/CBO9780511535581>.
- [16] Miyashiro A (1978) Nature of alkali volcanic rock series. *Contributions to Mineralogy and Petrology* 66, 91-104. <https://doi.org/10.1016/j.gr.2012.02.016>.
- [17] Ngako V & Njonfang E (2011) Plates amalgamation and plate destruction, the Western Gondwana history in *Tectonics* (D Closson Ed.), INTECH UK, pp. 3-34. <https://doi.org/10.5772/13518>.
- [18] Ngako V, Affaton P & Njonfang E (2008) Pan-African tectonics in northwestern Cameroon: implication for the history of western Gondwana. *Gondwana Research*, 14, 509-522. <https://doi.org/10.1016/j.gr.2008.02.002>.
- [19] Ngako V, Njonfang E, Tongwa AT, Affaton P & Nnange JM (2006) The North-South Paleozoic to Quaternary trend of alkaline magmatism from Niger-Nigeria to Cameroon: complex interaction between hotspots and Precambrian faults. *Journal of African Earth Sciences* 45, 241-256. <https://doi.org/10.1016/j.jafrearsci.2006.03.003>.
- [20] Ngounouno I, Déruelle B, Guiraud R, Vicat JP (2001) Magmatismes tholéïtite et alcalin des demi-grabens crétacés de Mayo Oulo-Léré et de Babouri-Figuil (Nord du Cameroun-Sud du Tchad) en domaine d'extension continentale. *Comptes Rendus de l'Académie des Sciences Paris* 333 (4), 201-207. [https://doi.org/10.1016/S1251-8050\(01\)01626-3](https://doi.org/10.1016/S1251-8050(01)01626-3).
- [21] Pearce JA (1982) Trace element characteristics of lavas from destructive plate boundaries. In *Andesites* (Thorpe RS, Ed.). John Wiley & Sons, New York, pp. 525-548. <http://orca.cardiff.ac.uk/id/eprint/8625>
- [22] Pearce JA (2008) Geochemical fingerprinting of oceanic basalts with applications to ophiolite classification and the search for Archean oceanic crust. *Lithos* 100, 14-48. <https://doi.org/10.1016/j.lithos.2007.06.016>.
- [23] Poudjom Djomani YH, Diament M, Wilson M (1997) Lithospheric structure across the Adamawa plateau (Cameroun) from gravity studies. *Tectonophysics* 273 (3-4), 317-328. [https://doi.org/10.1016/S0040-1951\(96\)00280-6](https://doi.org/10.1016/S0040-1951(96)00280-6).
- [24] Srivastava RK (2011) *Dyke Swarms: Keys for Geodynamic Interpretation*. Springer-Verlag: Berlin. <https://doi.org/10.1007/978-3-642-12496-9>.
- [25] Sun S-S & McDonough WF (1989) Chemical and isotopic systematics of oceanic basalts: implications for mantle composition and processes. *Geological Society of London Special Publications* 42, 313-345. <https://doi.org/10.1144/GSL.SP.1989.042.01.19>.
- [26] Tchakounté J, Eglinger A, Toteu SF, Zeh A, Nkoumbou C, Mvondo-Ondoa J, Penaye J, De Wit M & Barbey P (2017) The Adamawa-Yadé domain, a piece of Archean crust in the Neoproterozoic Central African Orogenic Belt (Bafia area, Cameroon). *Precambrian Res.* 299, 210-229. <https://doi.org/10.1016/j.precamres.2017.07.001>.
- [27] Toteu SF (1990) Geochemical characterization of the main petrographical and structural units of Northern Cameroon: implications for Pan-African evolution. *Journal of African Earth Sciences* 10 (4), 615-624. [https://doi.org/10.1016/0899-5362\(90\)90028-D](https://doi.org/10.1016/0899-5362(90)90028-D).
- [28] Toteu SF, Michard A, Bertrand JM & Rocci G (1987) U/Pb dating of Precambrian rocks from northern Cameroon, orogenic evolution and chronology of the Pan-African belt of Central Africa. *Precambrian Research* 37 (1), 71-87. [https://doi.org/10.1016/0301-9268\(87\)90040-4](https://doi.org/10.1016/0301-9268(87)90040-4).
- [29] Toteu SF, Penaye J, Deloué E, Van Schmus WR & Tchameni R (2006) Diachronous evolution of volcano-sedimentary basins north of the Congo craton: Insights from U–Pb ion microprobe dating of zircons from the Poli, Lom and Yaounde, Groups (Cameroon). *Journal of African Earth Sciences* 44, 428-442. [https://doi.org/10.1016/S0301-9268\(00\)00149-2](https://doi.org/10.1016/S0301-9268(00)00149-2).
- [30] Toteu SF, Penaye J, Poudjom Djomani Y (2004) Geodynamic evolution of the Pan-African belt in Central Africa with special reference to Cameroon. *Canadian Journal of Earth Sciences* 41 (1), 73-85. <https://doi.org/10.1139/e03-079>.
- [31] Toteu SF, Van Schmus WR, Penaye J & Michard A (2001) New U-Pb and Sm-Nd data from north-central Cameroon and its bearing on the pre-Pan African history of central Africa. *Precambrian Research* 108 (1-2), 45-73 [https://doi.org/10.1016/S0301-9268\(00\)00149-2](https://doi.org/10.1016/S0301-9268(00)00149-2).
- [32] Toteu SF, Van Schmus WR, Penaye J & Nyobé JB (1994) U-Pb and Sm-Nd evidence for Eburnean and Pan-African high-grade metamorphism in cratonic rocks of southern Cameroon. *Precambrian Research* 67, 321-347. [https://doi.org/10.1016/S0301-9268\(00\)00149-2](https://doi.org/10.1016/S0301-9268(00)00149-2).
- [33] Wang K, Plank T, Walker JD, Smith EI (2002) A mantle melting profile across the Basin and Range, SW USA. *Journal of Geophysical Research* 107 (ECV 5-1–ECV), 5-21. <https://doi.org/10.1029/2001JB000209>.
- [34] Wilson M & Guiraud R (1992) Magmatism and rifting in Western and Central Africa, from Late Jurassic to Recent times. *Tectonophysics* 213, 203-225. [https://doi.org/10.1016/0040-1951\(92\)90259-9](https://doi.org/10.1016/0040-1951(92)90259-9).
- [35] Wood DA (1980) The Application of a TH-HF-TA diagram to problems of tectonomagmatic classification and to establishing the nature of crustal contamination of basaltic lavas of the british tertiary volcanic province. *Earth and Planetary Science Letters* 50, 11-30. [https://doi.org/10.1016/0012-821X\(80\)90116-8](https://doi.org/10.1016/0012-821X(80)90116-8).